Shear Orientation of a Hexagonal Lyotropic Triblock Copolymer Phase As Probed by Flow Birefringence and Small-Angle Light and Neutron Scattering

Gudrun Schmidt and Walter Richtering*

Institut für Makromolekulare Chemie, Albert-Ludwigs-Universität Freiburg, Stefan Meierstrasse 31, D-79104 Freiburg, Germany

Peter Lindner

Institut Laue-Langevin, BP 156, F-38042 Grenoble, France

Paschalis Alexandridis

Department of Chemical Engineering, SUNY at Buffalo, Buffalo, New York 14260-4200, and Physical Chemistry 1, Center for Chemistry and Chemical Engineering, Lund University, P.O. Box 124, S-22100 Lund, Sweden

Received September 15, 1997; Revised Manuscript Received January 21, 1998

ABSTRACT: The shear orientation of the hexagonal liquid crystalline phase of a poloxamer-type triblock copolymer (poly(ethylene oxide)-*b*-poly(propylene oxide)-*b*-poly(ethylene oxide) (Pluronic L64))/water mixture was investigated by means of different techniques, namely, flow birefringence (Δn), small-angle light scattering, and small-angle neutron scattering (SALS, SANS). The evolution of birefringence is discussed for different types of shear. Oscillatory shear showed that birefringence displayed small oscillations during the first cycles until the sample was shear aligned. Then the same Δn value was obtained as in creep experiments. The degree of orientation depended on the strain. On a microscopic length scale probed by SANS, the shear flow results in an alignment of rodlike micelles along the flow direction. SANS experiments with the incident beam along the flow direction revealed that the 10 plane of the hexagonal lattice was aligned parallel to the flow-vorticity plane. On a mesoscopic length scale, studied by microscopy and SALS, a stripe texture was observed. SALS showed that the texture was similar to that obtained in low molar mass surfactants.

Introduction

Block copolymers are known to form structured phases both in the melt[1] and in solutions of selective solvents.[2,3] These phases are characterized by long-range orientation correlations when anisometric species are present and are then called liquid crystalline phases. Often a phase is observed that consists of a hexagonal packing of rodlike micelles. Liquid crystalls can be characterized by a director orientation. Samples of macroscopic size, however, are usually not uniformly aligned, and a polydomain structure is present. This polydomain structure gives rise to textures that can be observed by polarizing microscopy. The texture is characteristic of the mesophase structure and independent of the molecular structure; i.e., similar textures are found in lyotropic phases of copolymers and low molecular weight surfactants.[4,5] Amphiphilic block copolymers that form mesophases in concentrated aqueous mixtures are of special interest.[6−12] Amphiphilic block copolymers are intermediate between polymer melts on one hand and aqueous solution of low molar mass surfactants on the other hand. They are also interesting for practical applications.[13,14] This class of materials is a rather new field of research, and phase diagrams of many different systems have been reported recently.[9,15,16] However, only few papers have reported on the influence of shear on triblock copolymer lyotropic mesophases.[7,17−19]

* To whom correspondence should be sent. E-mail: rich@uni-freiburg.de.

The structure of liquid crystalline materials can be strongly affected by shear deformation. Often complicated flow properties are found and different behavior is observed as shear alignment or director tumbling can occur.[5,20−22] Shear-induced structural changes in complex fluids of anisotropic species are a very general problem encountered not only in block copolymer mesophases but also in liquid crystalline solutions of stiff macromolecules, thermotropic liquid crystals, and microemulsions.[20−25] Different experimental techniques as, e.g., flow birefringence, small-angle scattering and nuclear magnetic resonance from samples under shear have been developed in order to monitor such shear induced structural changes.[26−28] Since shear flow can influence both the texture and the orientation of the underlying anisotropic species, it is very helpful to combine different techniques in order to obtain information on different length scales.[29,30]

Block coplymer melts with hexagonal structure have been studied in great detail by many groups.[25] Often scattering techinques were used to investigate shear induced structural changes but also electron microscopy is feasible since the structure can be quenched easily. Often the 10 plane was found to be aligned parallel to shear plane given by flow and vorticity direction.[21,31−33] (the third Miller index is ommited because the rods are infinitely long) However, different orientations were found in large amplitude oscillatory shear as a function of temperature.[33]

The objective of this contribution is to investigate the influence of shear on the structure of the lyotropic

S0024-9297(97)01363-6 CCC: $15.00
Published on Web 03/20/1998

hexagonal phase of a triblock copolymer. Here a high amount of water is present and quenching of the structure for electron microscopy studies is much more complicated as compared to block copolymer melts. Therefore shear-induced structural changes have to be monitored in situ. Here we compare results obtained from different techniques: birefringence, small-angle light scattering (SALS), neutron scattering (SANS), and optical microscopy.

Experimental Section

The hexagonal phase of the triblock copolymer (poly(ethylene oxide)-*b*-poly(propylene oxide)-*b*-poly(ethylene oxide) $EO_{13}PO_{30}EO_{13}$, commercially available from BASF Corp. as Pluronic L64, was studied. A solution of 53% (w/w) in D_2O was prepared which had an isotropic to hexagonal phase transition at ca. 20 °C. The hexagonal region in the L64−water system is an "island" encircled by an isotropic polymer solution.[9] For all the different types of measurements, the shear cells were loaded with the sample being in the isotropic phase, and then the material was heated into the hexagonal phase. All experiments described below were started with a polydomain sample.

SALS and birefringence experiments were performed with a homemade device consisting of a Bohlin stress rheometer with either integrated light scattering or a birefringence setup. It is equipped with a 4 cm (diameter)/3° cone-and-plate shear geometry. The incident beam was parallel to the velocity gradient, and the sample thickness probed by the laser beam was 0.78 mm. Both polarized and depolarized scattering can be detected. Here only results from depolarized scattering (H_v) will be discussed. The largest accessible scattering vector was 3 μm^{-1}. A detailed description is given elsewere.[34]

The determination of flow birefringence is based on a method described by Lim and Ho.[35] The light beam was parallel to the direction of the velocity gradient. It is useful to define the retardation δ when the birefringence Δn is detected by means of the different velocities of the light along the two orthogonal axes for the refractive indices n_1 and n_2 ($\Delta n = n_1 - n_2$). Then the electric vector of the incoming light has to point into the direction of both axes, and this can be realized by linear polarized light, with a direction of polarization at 45° to both axes. The retardation δ is the phase difference of both beams after passing through a material of the thickness d and is defined by the equation

$$\delta = 2\pi\frac{d\Delta n}{\lambda} \tag{1}$$

The effect of the optical elements and the retardation of the sample on the measured intensity (with Θ being the rotation angle between the analyzer and polarizer) can be calculated with Stokes vectors and Müller matrixes.[28,36] The resulting intensity $I_{res}(\Theta,\delta)$ is

$$I_{res}(\Theta,\delta_{meas}) = I_0A(1 + \cos(2\Theta - \delta_{meas})) \tag{2}$$

where A is the scaling factor which takes into account an absorption of light. The phase angle δ_{meas} (retardation) is measured as follows: using a plate with two 90° chopper segments the rotating analyzer interrupts a light barrier two times on each rotation. Thus one obtains the phase angle δ from the *cos* $(2\Theta - \delta)$ of the measured intensity and the chopper signal at $\Theta = 0$, 90, 180, 270°, etc. from the rotating analyzer. The retardation of the probe is given as multiples of 2π, and the number of orders has to be taken into account in order to calculate the correct value of birefringence. Since the sample thickness in the cone-and-plate shear geometry is much smaller as compared to that in concentric cylinders, the number of orders is only a problem when strongly birefringent samples are investigated. A further advantage of the cone-and-plate setup as compared to using a couette cell is the smaller inertia of the cone that allows one to perform dynamic-mechanical experiments within a broad frequency range.[37]

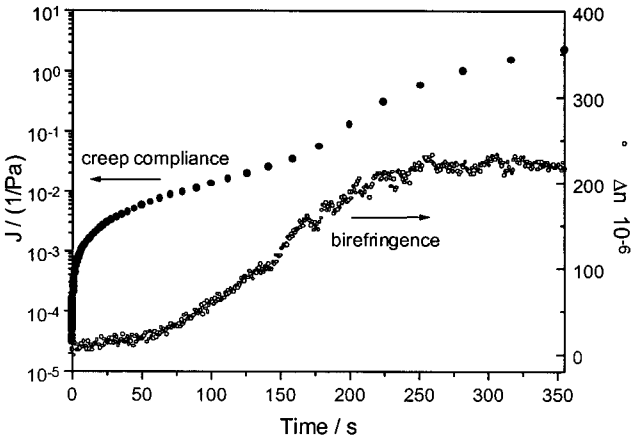

Figure 1. Creep compliance (●) vs time at a stress of σ = 100 Pa and the simultaneously measured birefringence (○).

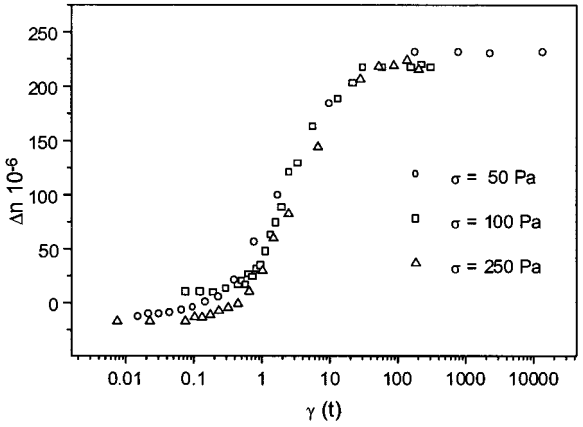

Figure 2. Birefringence Δn as a function of strain from creep experiments for three different stresses: σ = 50 Pa (○); σ = 100 Pa (□); σ = 250 Pa (△).

SANS measurements were performed using the instrument D11 at the Institute Laue-Langevin Grenoble. The couette type shear cell has a gap of 1 mm. In the standard configuration called the "radial beam" geometry the incident beam is aligned parallel to the shear gradient. A second configuration is the "tangential beam", where the beam enters the couette cell tangentially, i.e., along the flow direction. The q range is $0.11 < q < 1.48$ nm^{-1} for the "radial beam" geometry and $0.11 < q < 2.23$ nm^{-1} for the "tangential beam" configuration. q is the magnitude of the scattering vector given as $q = 4\pi/\lambda \sin(\theta)/2$. λ and θ are the radiation wavelength (4.5 Å) and scattering angle, respectively. A detailed description of the shear cell was given elsewere.[38,39]

Results and Discussion

Rheo-birefringence. A series of creep experiments was performed at constant temperature but different shear stresses. The development of shear-alignment was recorded in real time using flow-birefringence. Figure 1 shows the time dependent compliance $J(t) = \gamma(t)/\sigma$ and birefringence in one of these creep experiments at a shear stress of σ = 100 Pa. The birefringence increased until a plateau of $\Delta n = (0.22 \pm 0.01) \times 10^{-3}$ was reached. No recoverable strain could be detected after cessation of shear, and the birefringence value remained constant. Additional measurements were performed at 10, 50, 150, and 250 Pa, respectively. Figure 2 shows a good overlap of Δn as a function of strain (γ) for creep experiments at three different

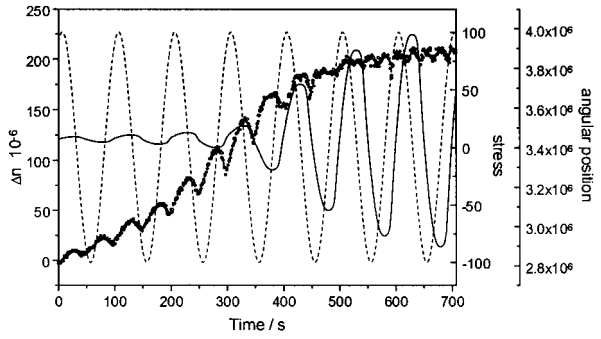

Figure 3. Oscillatory shear experiment at a frequency of 0.01 Hz and a maximum stress of 100 Pa. Stress (- - -), angular position of the cone (—), and birefringence (○) are given as a function of time.

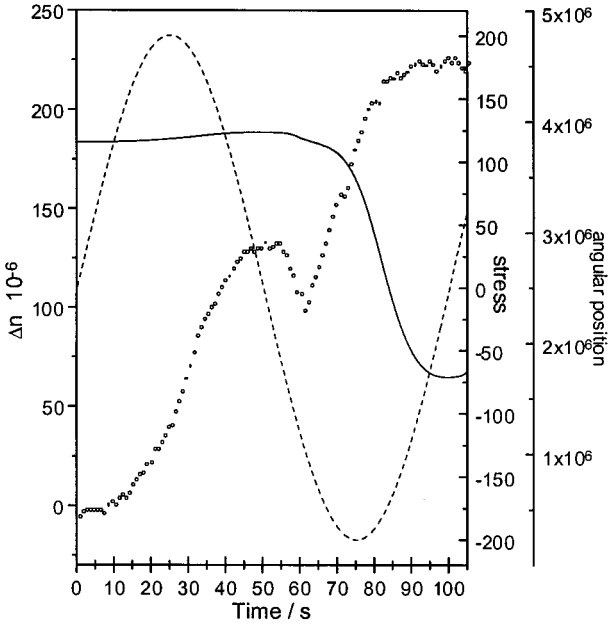

Figure 4. Oscillatory shear experiment at a frequency of 0.01 Hz and a maximum stress of 200 Pa. Stress (- - -), angular position of the cone (—), and birefringence (○) are given as a function of time.

stresses. The same plateau value was found after ca. 40 strain units. Obviously shear alignment depended on strain, similar to the behavior of hexagonal phases of low molecular weight surfactants.[39]

Results from oscillatory shear are summarized in Figures 3 and 4. Three curves are shown: (i) the applied stress, (ii) the angular position of the cone representing the deformation, and (iii) birefringence. Figure 3 displays data from a time sweep experiment at a frequency of 0.01 Hz and a maximum stress of 100 Pa. A constant birefringence value of $\Delta n = (0.22 \pm 0.01) \times 10^{-3}$ was found after five cycles, indicating that oscillatory shear lead to the same degree of orientation as the creep experiments discussed above. With a shear stress of 200 Pa, the sample was aligned in only one cycle; see Figure 4. The birefringence data in Figure 3 and 4 show small oscillations during the first few cycles. The local maxima of the Δn curve are correlated to the extrema of the strain curve; i.e., the shear alignment depended on strain in agreement with creep experiments. During the first few cycles, the change of flow direction reduced the orientation at first. However, once the sample was shear aligned, flow reversal did not alter the degree of orientation anymore. Figure 3 shows that

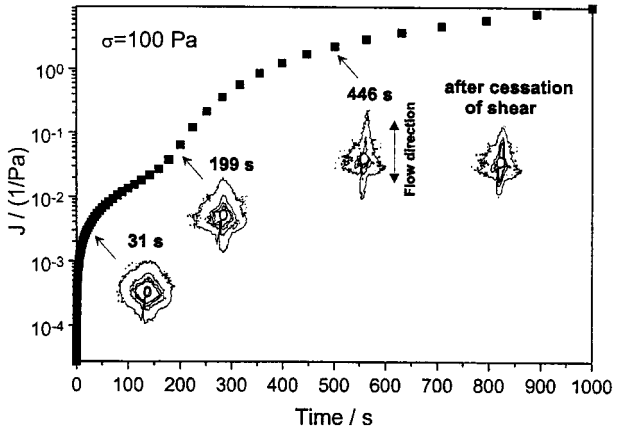

Figure 5. Creep compliance (■) vs time at a stress of σ = 100 Pa and simultaneously detected depolarized scattering patterns after (a) 31 s, (b) 199 s, (c) 446 s and (d) the relaxation pattern 7 min after cessation of shear.

the strain amplitude increased although the maximum stress amplitude was kept constant. Thus the moduli decreased and the material became softer with increasing shear alignment. The same behavior can be seen in the creep curve (Figure 1). The creep compliance increased strongly when the sample became aligned. The rheological data displayed in Figures 1−3 demonstrate that the shear aligned hexagonal phase has lower moduli as compared to the polydomain sample. The rheological behavior of the triblock copolymer sample is therefore very similar to the behavior observed with the hexagonal phase of low molecular weight surfactants.[40,41] However, the strain necessary to obtain the birefringence plateau was larger as compared to common surfactants.[39]

Small-Angle Light Scattering and Optical Microscopy. Depolarized light scattering was performed in order to obtain information on the evolution of texture during shear flow.

After the sample was heated into the hexagonal phase at 25 °C, a symmetrical depolarized scattering pattern was observed with the sample in the quiescent state. The corresponding micrograph from polarizing microscopy under crossed polarizers showed small birefringent domains with nonbirefringent parts in between. Size and number of birefringent domains increased with annealing time. This is in contrast to low mass surfactants where a distinct hexagonal texture is observed immediately after the phase transition. Thus the cristallization time of the triblock copolymer phase is much longer as compared to low molar mass surfactants.[3]

Figure 5 displays SALS patterns and compliance in a creep experiment at a shear stress of $\sigma = 100$ Pa. The first three SALS patterns, a−c, in the plot show characteristic depolarized scattering patterns taken simultaneous to the creep curve. Scattering was obtained along the flow direction. The SALS patterns showed no sharp transition when the jump in the creep compliance occurred, but the anisotropy of the intensity distribution increased with time. The observed depolarized scattering pattern with enhanced intensity along the flow direction corresponds to a stripe texture in polarizing microscopy, where stripes perpendicular to the flow direction are found. The stripe texture is caused by an undulation of the director which on average is oriented along the flow direction.[39,42,43] SALS measurements after cessation of shear showed an

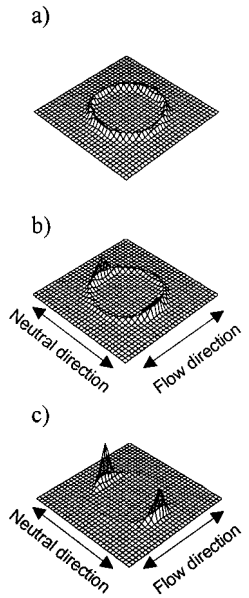

Figure 6. SANS patterns obtained with the "radial" beam configuration: (a) sample cooled into the hexagonal phase; at rest prior to shear; (b, c) scattering pattern at a strain of (b) $\gamma = 12$ and (c) $\gamma = 135$. q-range: $0.11 < q < 1.48$ nm^{-1}.

increased and sharper scattering intensity (Figure 5d) indicating an improvement of order on the micrometer length scale. When a constant stress experiment was repeated with a presheared sample, the SALS intensity dropped again but recovered when shear flow was stopped.

Optical micrographs of a sample, ca. 30−120 min after cessation of shear showed thinner and more aligned stripes than those obtained during and directly after shear flow. In other words a refinement of texture was observed after cessation of shear, indicating an increase of order on the micrometer length scale.

Small-Angle Neutron Scattering. Two beam configurations were used in small-angle neutron scattering as outlined in the Experimental Section. Results obtained from the hexagonal phase with the "radial" beam (i.e. the neutron beam was parallel to the velocity gradient) are summarized in Figure 6. A Bragg-peak caused by the local order of the rodlike micelles was observed on the two-dimensional multi-detector at $q_{max} = 0.8$ nm^{-1}. This value is in agreement with X-ray scattering data and is correlated with the 10 plane of the hexagonal lattice.[9] The two-dimensional scattering pattern was radially symmetric when the sample was in the quiescent state. A symmetric intensity distribution is typical of a polydomain sample where all spatial orientations of domains of rodlike micelles are present.

An anisotropic scattering pattern developed with the sample under shear and did not change directly after cessation of shear. The Bragg peak was only observed perpendicular to the flow direction, showing that the rodlike micelles were aligned along the flow direction. The same behavior was observed from other lyotropic block copolymers[44] and from different surfactant systems.[39,45]

The sample was sheared at constant rate for certain time intervals and scattering patterns were recorded immediately after cessation of shear. To quantify the anisotropy of the scattering pattern, two procedures were used: (i) the integrated scattering intensity was determined from 30°-sectors perpendicular to and along

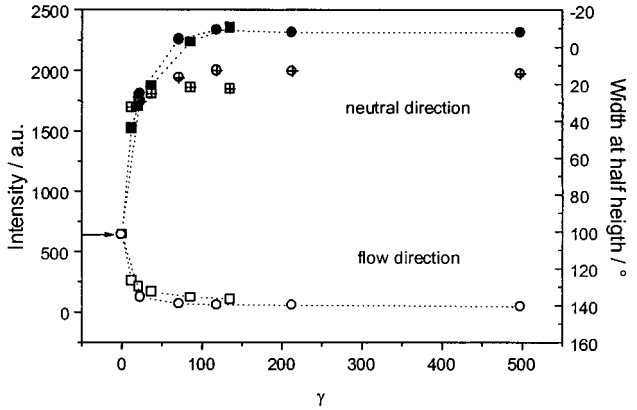

Figure 7. Integrated SANS intensity from 30° sectors perpendicular to (●, ■) and parallel to (□, ○) the flow direction plotted vs strain γ for experiments at two different shear rates: (■, □) $d\gamma/dt = 0.82$ s^{-1}; (●, ○) $d\gamma/dt = 4.74$ s^{-1}. Width at half-maximum obtained from a Laurenzian fit of the azimuthal trace of scattering intensity: $d\gamma/dt = 0.82$ s^{-1} (crossed square) and $d\gamma/dt = 4.74$ s^{-1} (crossed circle).

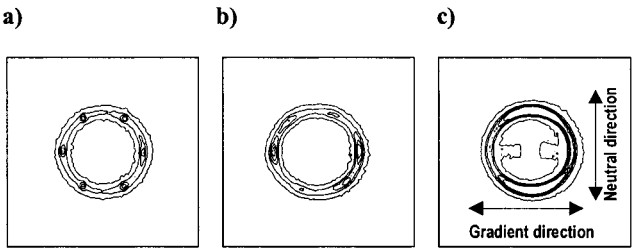

Figure 8. Two-dimensional SANS profiles obtained with the "tangential" beam (a) at rest, immediately after heating into the hexagonal state (19 °C), (b) at rest at 24 °C, and (c) from a sheared sample. q-range: $0.11 < q < 1.48$ nm^{-1}.

the flow direction: (ii) the azimuthal trace of the scattering intensity was fitted to a Lorentzian to obtain the width at half-maximum. Results from experiments at two shear rates, 0.82 and 4.74 s^{-1}, respectively, are displayed in Figure 7 as a function of strain. Obviously a constant degree of orientation was reached after ca. 40 strain units in agreement with results from flow birefringence.

SANS data obtained with the "tangential" beam (i.e. the neutron beam was along the flow direction) are shown in Figure 8. When heating the sample from the isotropic into the hexagonal state a 6-fold symmetry (Figure 8a) was observed immediately after the phase transition occurred at 19 °C. The pattern indicates the presence of a small amount of highly oriented hexagonal parts in the sample. This effect is due to the geometry of the shear cell's temperature control unit and is described elsewere.[39] The scattering pattern shown in Figure 8b was observed at 24 °C. The distribution of scattering intensity was now nearly isotropic which confirms the long cristallization time observed in optical microscopy. Under shear strong scattering intensity was observed in the neutral direction (Figure 8c). The q_{max} position of the first-order peak is identical to that determined with the "radial beam" setup. Then, 45 min after cessation of shear, we obtained a relaxation pattern such as that shown in Figure 9. Here the sample to detector distance was reduced, giving access to larger scattering vectors. A 6-fold symmetry and even third-order reflections can be seen in Figure 9. The angular dependence of the scattering intensity is shown in Figure 10. Here the intensity of two different sectors

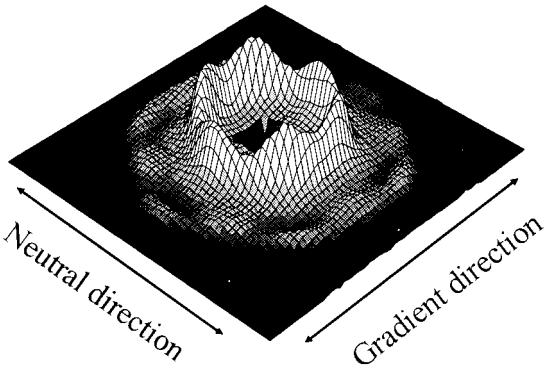

Figure 9. Three-dimensional SANS profile obtained with the "tangential" beam, 45 min after cessation of shear. The logarithm of intensity is shown to increase the visibility of the second- and third-order peaks. q-range: $0.11 < q < 2.23$ nm^{-1}.

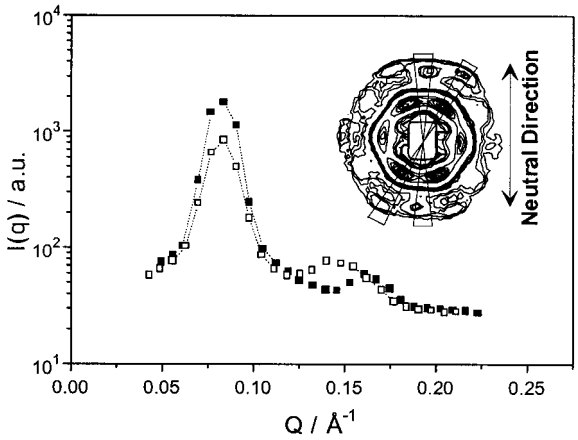

Figure 10. SANS profile obtained 45 min after shearing and q-dependence of SANS scattering intensity averaged in neutral direction (□) and 30° to neutral direction (■).

Table 1. Peak Positions Obtained by SANS and SAXS[9] from the Hexagonal Phase

	q_1/Å^{-1}	q_2/Å^{-1}	q_3/Å^{-1}
SANS	0.084	0.140	0.161
SAXS	0.077	0.133	0.155

on the two-dimensional multidetector are displayed: (i) a sector along the neutral direction (□) and (ii) a sector 30° off the neutral direction (■), as indicated in the contour plot also shown in Figure 10. The q_{max} positions of the three peaks are summarized in Table 1 and agree well with X-ray scattering data. The positions of the scattering peaks show that the 10 plane of the hexagonal lattice was aligned parallel to plane given by the flow and vorticity direction (shear plane); see Figure 11. However, the alignment was not perfect because the 10 reflection was also observed in the radial beam experiment.

The 6-fold symmetry shown in Figure 9 was only observed after cessation of shear. During shear and directly after stopping the shear flow, however, only broad reflections were observed in the vorticity direction; see Figure 8c. Apparently the rotational component of the flow field destroyed the 6-fold symmetry as was also reported in the case of polymer melts.[22] A similar observation was made with the "radial beam": the intensity of the second-order peak increased after cessation of shear. This indicates that the hexagonal phase under shear has a reduced degree of order and forms a layered structure which is observable in the radial and tangential beam configuration. After shear,

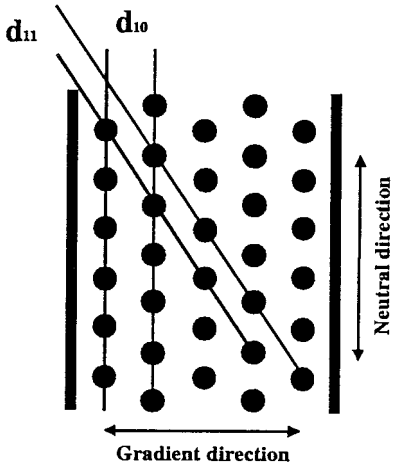

Figure 11. Real space orientation of sheared micelles in the couette cell.

the 6-fold symmetry is recovered, as is seen with the tangential beam. Remnants of the layers, however, lead to a high intensity and a broadening of the reflections in the neutral direction (Figure 10). Apparently they also dominated the scattering pattern observed with the radial beam.

The experimental results show that the lyotropic hexagonal phase of the amphiphilic triblock copolymer behaves similar to hexagonal phases of block copolymer melts and of common surfactants. However the influence of shear on these polymer micelles is different as compared to lyotropic nematic phases of stiff rodlike macromolecules as, e.g., (hydroxypropyl)cellulose, HPC, or poly(benzylglutamate), PBG. These systems have been intensively studied during the last years,[46,47] and a comparison of results obtained from similar experimental techniques as used in this contribution was given recently by Burghardt and co-workers.[48] In contrast to the block copolymer hexagonal phase, the degree of orientation in the lyotropic nematic polymer solutions depends on shear rate. Three different regimes can be obtained as a function of shear rate: (i) a texture dominated flow, (ii) director tumbling, and (iii) flow alignment at high shear rates. The degree of orientation usually decreases after cessation of shear; again a different behavior is observed here with the hexagonal phase, as was discussed above.

Concerning the experimental techniques, our results agree with the data by Burghardt and co-workers.[48] Birefringence and SANS data provide a consistent description of the evolution of orientation under shear. The study by Hongladarom et al.[48] nicely demonstrated that different procedures for the evaluation of small angle scattering data, as, e.g., peak intensity, width at half-height, alignment factor, and order parameter, provide equivalent information on the shear induced order. Therefore we only used peak intensity and width at half-height. The calculation of the order parameters was somewhat arbitrary due to problems in baseline correction.[49] Therefore we only determined the order parameters for the aligned sample and obtained ca. $P_2 = 0.8$.

In depolarized *small-angle light* scattering, different scattering patterns are observed in lyotropic hexagonal and nematic phases, respectively. This is correlated to different textures. The shear-aligned hexagonal phase is characterized by a director undulation along the flow direction. This gives rise to a stripe texture with stripes perpendicular to the flow direction; thus, enhanced

depolarized light scattering is observed *along* the flow direction. However, depolarized SALS from nematic phases is characterized by a high scattering intensity *perpendicular* to the flow direction. This streak is sometimes modulated, corresponding to a banded texture.[47]

Conclusions

The results presented above provide clear information on the shear orientation of the micellar hexagonal triblock copolymer phase. On a microscopical length scale probed by SANS, the shear flow resulted in an alignment of rodlike micelles along the flow direction, and the 10 plane of the hexagonal lattice was parallel to the shear plane. This behavior is similar to that of polymer melts and solutions of low molar mass surfactants.[21,31−33,39] Small-angle light scattering, however, provides information on the evolution of texture under flow. Here, scattering along the flow direction was observed corresponding to a stripe texture with stripes perpendicular to the flow direction.[39] The degree of shear alignment depends on strain, and rheo-birefringence data showed that simple shear and large amplitude oscillatory shear give the same results.

The behavior of the lyotropic hexagonal phase of the PEO−PPO−PEO triblock copolymer under shear is thus very similar to that of low molar mass surfactants and block copolymer melts.

Acknowledgment. Support by the Deutsche Forschungsgemeinschaft is gratefully acknowledged.

References and Notes

(1) Bates, F. S.; Schulz, M. F.; Khandpur, A. K.; Förster, S.; Rosedale, J. H.; Almdal, K.; Mortensen, K. *Faraday Discuss.* **1994**, *98*, 7.
(2) Gast, A. P. *Langmuir* **1996**, *12*, 4060.
(3) Alexandridis, P.; Olsson, U.; Lindman, B. *Langmuir* **1997**, *13*, 23.
(4) Lühmann, B.; Finkelmann, H. *Colloid Polym. Sci.* **1987**, *265*, 506.
(5) Chandrasekhar, S. *Liquid Crystals*, 2nd ed.; Cambridge University Press: Cambridge, England, 1992.
(6) Mortensen, K.; Brown, W.; Almdal, K.; Alami, E.; Jada. A. *Langmuir* **1997**, *13*, 3635.
(7) Mortensen, K.;*Europhys. Lett.* **1992**, *19*, 599.
(8) Zhang, K.; Khan, A. *Macromolecules* **1995**, *28*, 3807.
(9) Alexandridis, P.; Zhou, D.; Khan, A. *Langmuir* **1996**, *12*, 2690.
(10) Prud'homme, R. K.; Wu, G.; Schneider, D. K. *Langmuir* **1996**, *12*, 4651.
(11) Alexandridis, P. *Curr. Opin. Colloid Interface Sci.* **1997**, *2*, 478.
(12) Almgreen, M.; Brown, W.; Hvid, S. *Colloid Polym. Sci.* **1995**, *273*, 2.
(13) Rounds, R.; S. *Surfactant Sci. Ser.* **1997**, *67*, 67.
(14) Alexandridis, P. *Curr. Opin. Colloid Interface Sci.* **1996**, *1*, 490.
(15) Glatter, O.; Scherf, G.; Schiller, K.; Brown, W. *Macromolecules* **1994**, *27*, 6046.
(16) Wanka, G.; Hoffmann, H.; Ulbricht, W. *Macromolecules* **1994**, *27*, 4.
(17) Berret, J. F.; Molino, F.; Porte, G.; Diat, O.; Lindner, P. *J. Phys. Condens. Matter.* **1996**, *8*, 9513.
(18) Diat, O.; Porte, G.; Berret, J. F. *Phys. Rev. B* **1996**, *54*, 14869.
(19) Slawecki, T. M.; Glinka, C. J. Presented at the ACS Colloid Surface Science Symposium, Newark, DE 1997.
(20) Marruci, G.; Greco, F. *Adv. Chem. Phys.* **1993**, *86*, 331.
(21) Jamieson, A. M.; Gu, D. F.; Chen, F. L.; Smith, S. *Prog. Polym. Sci.* **1996**, *2185*, 981.
(22) Nakatani, A. I.; Morrison, F. A.; Jackson, C. L.; Douglas, J. F.; Mays, J. W.; Muthukumar, M.; Han, C. C. *J. Macromol. Sci.—Phys.* **1996**, *B35*, 489.
(23) Hadziioannou, G.; Mathis, A.; Skoulios, A. *Colloid Polym. Sci.* **1979**, *257*, 136.
(24) Bates, F. S.; Koppi, K. A.; Tirrel, M.; Almdal, K.; Mortensen, K. *Macromolecules* **1994**, *27*, 5934.
(25) Fredrickson, G. H.; Bates, F. S. *Annu. Rev. Mater. Sci.* **1996**, *26*, 501.
(26) Larson, R. G. *Rheol. Acta* **1992**, *31*, 497.
(27) Grabowski, D. A.; Schmidt, C. *Macromolecules* **1994**, *27*, 2632.
(28) Fuller, G. G. *Optical Rheometry of Complex Fluids*; Oxford University Press: Oxford, England, 1995.
(29) Safinja, C. R.; Sirota, E. B.; Bruinsma, F.; Jeppesen, C.; Plano, R.; Wenzel, L. *Science* **1993**, *61*, 588.
(30) Richtering, W. *Prog. Colloid Polym. Sci.* **1997**, *104*, 90.
(31) Almdal, K.; Bates, F. S.; Mortensen, K. *J. Chem. Phys.* **1992**, *96*, 9122.
(32) Winter, H. H.; Scott, D. B.; Gronski, W.; Okamoto, S.; Hashimoto, T. *Macromolecules* **1993,** *26*, 7236.
(33) Tepe, T.; Schulz, M. F.; Zhao, J.; Tirrell, M.; Bates, F. S.; Mortensen, K.; Almdal, K. *Macromolecules* **1995**, *28*, 3008.
(34) Berghausen, J.; Fuchs, J.; Richtering, W. *Macromolecules* **1997**, *30*, 7574.
(35) Lim, K. C.; Ho, J. T. *Mol. Cryst. Liq. Cryst.* **1978**, *47*, 173.
(36) Azzam, R. M. A.; Bashara, N. M. *Ellipsometry and Polarized Light*; North Holland: Amsterdam, 1987.
(37) Schmidt, J.; Weigel, R.; Richtering, W.; Burchard, W. *Macromol. Symp.* **1997**, *120*, 247.
(38) Lindner, P.; Oberthür, R. C. *Rev. Phys. Appl.* **1984**, *19*, 759.
(39) Schmidt, G.; Müller, S.; Lindner, P.; Schmidt, C.; Richtering, W. *J. Phys. Chem. B* **1998**, *102*, 507.
(40) Richtering, W.; Läuger, J.; Linemann, R. *Langmuir.* **1994**, *10*, 4374.
(41) Linemann, R.; Läuger, J.; Schmidt, G.; Kratzat, K.; Richtering, W. *Rheol. Acta* **1995**, *34*, 440.
(42) Müller, S.; Fischer, P.; Schmidt, C. *J. Phys. II Fr.* **1997**, *7*, 421.
(43) Oswald, P.; Geminard, J. C.; Lejcek, L.; Sallen, L. *J. Phys. II Fr.* **1996**, *6*, 281.
(44) Mortensen, K. *J. Phys Condens. Matter.* **1996**, *8*, A 103.
(45) Fairhurst, C. E.; Holmes, M. C.; Leaver, M. S. *Langmuir* **1996**, *12*, 6336.
(46) Walker, L. M.; Wagner, N. J. *Macromolecules* **1996**, *29*, 2298.
(47) Patlazahn, S. A.; Riti, J. B.; Navard, P. *Macromolecules* **1996**, *29*, 2029.
(48) Hongladarom, K.; Ugaz, V. M.; Cinader, D. K.; Burghardt, W. R.; Quintana, J. P.; Hsiao, B. S.; Dadmun, M. D.; Hamilton, W. A.; Butler, P. D. *Macromolecules* **1996**, *29*, 5346.
(49) Mitchell, G. R.; Windle, A. H. in *Developments in Crystalline Polymers*; Bassett, D. C., Ed.; Elsevier: London, 1988.

MA971363V